JOC Article

Theoretical Prediction of a Perepoxide Intermediate for the Reaction of Singlet Oxygen with *trans*-Cyclooctene Contrasts with the Two-Step No-Intermediate Ene Reaction for Acyclic Alkenes

Andrew G. Leach,[†] K. N. Houk,*[,‡] and Christopher S. Foote[§,‡]

AstraZeneca Pharmaceuticals, Mereside, Alderley Park, Macclesfield, Cheshire, U.K., and Department of Chemistry and Biochemistry, University of California, Los Angeles, California 90095-1569

houk@chem.ucla.edu

Received July 22, 2008

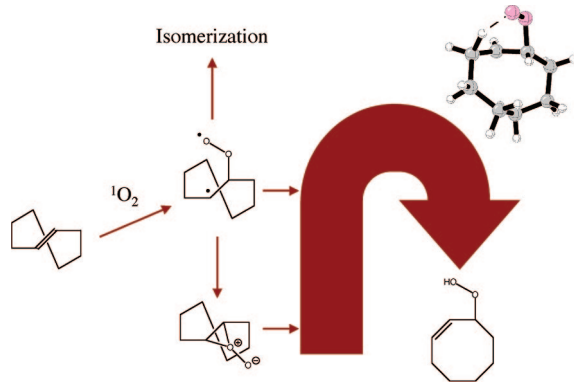

B3LYP/6-31G* and CASMP2 calculations have been employed to study the ene reaction of singlet oxygen with *trans*-cyclooctene. These methods predict that the reaction involves a perepoxide intermediate, whereas alkenes such as tetramethylethylene are predicted by the same methods to occur by a two-step no-intermediate mechanism, with no perepoxide intermediate. The change in mechanism arises because the *trans*-cyclooctene imposes a substantial strain in the transition state for hydrogen abstraction. The perepoxide is formed through a polarized diradical intermediate that can lead to the observation of alkene isomerization. The polarized diradical also becomes a minimum because of the barrier to abstraction.

Introduction

Theoretical studies of the ene reaction of singlet oxygen with tetramethylethylene have established a two-step no-intermediate mechanism for this reaction.[1] This conclusion overturns the long-held belief that perepoxide intermediates are formed in such reactions; experimental studies have demonstrated the existence of a perepoxide intermediate in a few cases. *trans*-Cyclooctene has a geometry that prevents allylic hydrogen abstraction, and consequently the perepoxide intermediate is expected to have a longer lifetime than in normal alkenes.[2] Indeed, this alkene gives a characterizable aziridine imide intermediate in the ene reaction with triazolinediones.[3]

The reaction of *trans*-cyclooctene with singlet oxygen has now been studied with a computational methodology that predicts no intermediate for the reaction of simple alkenes such as tetramethylethylene with singlet oxygen. Here we show that *trans*-cyclooctene and singlet oxygen give a perepoxide intermediate that is a genuine energy minimum. This is a consequence of the strain in the cyclooctene ring that constrains the allylic CH bonds to be positioned in inappropriate positions for abstraction. The mechanism calculated for this system is analogous to that calculated for the ene reaction of nitroso compounds and triazolinediones.[4] These DFT and CASMP2

[†] AstraZeneca Pharmaceuticals.
[‡] University of California, Los Angeles.
[§] Deceased, June 13, 2005.

(1) Singleton, D. A.; Hang, C.; Szymanski, M. J.; Meyer, M. P.; Leach, A. G.; Kuwata, K. T.; Chen, J. S.; Greer, A.; Foote, C. S.; Houk, K. N. *J. Am. Chem. Soc.* **2003**, *125*, 1319–1328.

(2) Poon, T. H. W.; Pringle, K.; Foote, C. S. *J. Am. Chem. Soc.* **1995**, *117*, 7611–7618.

(3) Poon, T. H. W.; Park, S. H.; Elemes, Y.; Foote, C. S. *J. Am. Chem. Soc.* **1995**, *117*, 10468–10473.

(4) (a) Leach, A. G.; Houk, K. N. *Chem. Commun.* **2002**, 1243–1255. (b) Leach, A. G.; Houk, K. N. *J. Am. Chem. Soc.* **2002**, *124*, 14820–14821. (c) Leach, A. G.; Houk, K. N. *Org. Biomol. Chem.* **2003**, 1389–1403. (d) Singleton, D. A.; Hang, C. *J. Am. Chem. Soc.* **1999**, *121*, 11885.

10.1021/jo8016154 CCC: $40.75 © 2008 American Chemical Society
Published on Web 10/04/2008

calculations provide a unifying view of the ene reactions of singlet oxygen and explain experimental observations.

Background

The ene reaction of singlet oxygen has been a long-standing mechanistic curiosity that has attracted the attention of many scientists.[5] At issue are the details of the order and nature of bond-forming and bond-breaking events. The reaction could in principle proceed through a concerted transition state like **1**, since the reaction is an allowed reaction according to the Woodward−Hoffmann orbital symmetry rules.[6] Alternatively, a range of stepwise processes through intermediates could take place. These intermediates may be the diradical **2**, zwitterion, **3**, perepoxide, **4**, 1,2-dioxetane, **5**, or peroxyl-allyl radical pair, **6/7**. Many experimental and theoretical studies have been undertaken. Frequently, a perepoxide is assumed[7] or inferred indirectly from stereoselectivity or isotope effects.[8,9] Most cases where a perepoxide has been shown to exist involve substrates that cannot undergo an ene reaction.[10] *trans*-Cyclooctene is an interesting case, because it can undergo the ene reaction, yet its geometry is unfavorable for the hydrogen abstraction. Upon reaction with triazolinedione, *trans*-cyclooctene gives an aziridine imine intermediate that is stable enough at low temperatures to be characterized by NMR.[3] In the singlet oxygen reaction, the product of the ene reaction is identifiable alongside products believed to be derived from trapping by phosphite of an unusually long-lived perepoxide.[2]

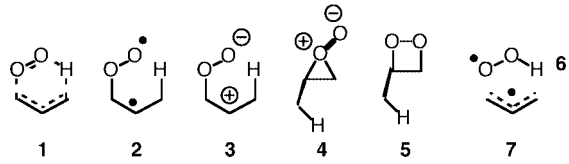

A collaborative effort between us and Daniel Singleton reported theoretical studies of the ene reaction of singlet oxygen with tetramethylethylene, (*Z*)-2-butene, and 2-methyl-2-butene.[1] A potential energy surface was found that can readily explain almost all of the experimental observations, notably kinetic isotope effects and the *cis*-effect,[11] whereby abstraction takes place preferentially from the most substituted side of an alkene. The mechanism that was calculated was styled "two-step no-intermediate" and is illustrated in Figure 1. An initial transition state **8** with the symmetry of a perepoxide is the first "step". Following along the symmetrical path from this transition state might lead to a minimum representing a perepoxide intermediate. Instead, this path leads to a second transition state resembling a perepoxide, **9**. This transition state is for a hypothetical process for translation of the O−O fragment from one terminus of the alkene to the other. The lowest energy path, however, is not symmetrical. At the point at which the symmetrical path ceases to be a valley and becomes a ridge, the second derivative of the energy orthogonal to the reaction path for one degree of freedom becomes zero (it is positive in the valley region and negative in the ridge region). This point has a zero vibrational frequency perpendicular to the principal reaction coordinate and is called a valley ridge inflection point.[12] The reaction path bifurcates in this region of the potential energy surface and proceeds downhill from the initial transition state **8** directly to products **10** or **10′** (related by symmetry). No-intermediate exists and the second transition state **9** is not directly sampled. The two-step no-intermediate mechanism can rationalize the experimental observations for simple alkenes. A dynamics study revealed that this potential energy surface can also reproduce experimentally observed kinetic isotope effects.[13]

This interpretation involves no perepoxide intermediate but a more loosely associated valley-ridge inflection region on the potential energy surface. However, there are a few cases of reactions of alkenes with singlet oxygen where perepoxide intermediates have apparently been trapped. One case is particularly striking: the reaction of *trans*-cyclooctene yields products derived from trapping of a perepoxide and ene products.[2,14] Other examples generally do not yield ene products.[10] We have investigated the *trans*-cyclooctene case theoretically, to determine if the two-step no-intermediate mechanism

(5) (a) Foote, C. S.; Wexler, S. *J. Am. Chem. Soc.* **1964**, *86*, 3879. (b) Corey, E. J.; Taylor, W. C. *J. Am. Chem. Soc.* **1964**, *86*, 3880. (c) Windaus, A.; Brunken, J. *Liebigs Ann. Chem.* **1928**, *103*, 225. (d) Kearns, D. R. *Chem. Rev.* **1971**, *71*, 395. (e) Prein, M.; Adam, W. *Angew. Chem., Int. Ed. Engl.* **1996**, *35*, 477.

(6) Woodward, R. B.; Hoffmann, R. *Angew. Chem., Int. Ed.* **1969**, *8*, 781 *The Conservation of Orbital Symmetry*; Verlag Chemie: Weinheim, 1970.

(7) (a) Stratakis, M.; Orfanopoulos, M.; Chen, J. S.; Foote, C. S. *Tetrahedron Lett.* **1996**, *37*, 4105–4108. (b) Elemes, Y.; Foote, C. S. *J. Am. Chem. Soc.* **1992**, *114*, 6044–6050. (c) Stratakis, M.; Orfanopoulos, M. *Tetrahedron Lett.* **1997**, *38*, 1067–1070. (d) Adam, W.; Klug, P. *J. Org. Chem.* **1993**, *58*, 3416–3420. (e) Linker, T.; Fröhlich, L. *J. Am. Chem. Soc.* **1995**, *117*, 2694–2697. (f) Dussault, P. H.; Zope, U. R. *Tetrahedron Lett.* **1995**, *36*, 2187–2190. (g) McCapra, F.; Beheshti, I. *J. Chem. Soc., Chem. Commun.* **1977**, 517–518. (h) Greer, A.; Vassilikogiannakis, G.; Lee, K.-C.; Koffas, T. S.; Nahm, K.; Foote, C. S. *J. Org. Chem.* **2000**, *65*, 6876–6878. (i) Vassilikogiannakis, G.; Stratakis, M.; Orfanopoulos, M.; Foote, C. S. *J. Org. Chem.* **1999**, *64*, 4130–4139. (j) Davis, K. M.; Carpenter, B. K. *J. Org. Chem.* **1996**, *61*, 4617–4622. (k) Adam, W.; Richter, M. J. *J. Org. Chem.* **1994**, *59*, 3335–3340.

(8) (a) Orfanopoulos, M.; Smonou, I.; Foote, C. S. *J. Am. Chem. Soc.* **1990**, *112*, 3607–3614. (b) Grdina, B.; Orfanopoulos, M.; Stephenson, L. M. *J. Am. Chem. Soc.* **1979**, *101*, 3111. (c) Kopecky, K. R.; van de Sande, J. H. *Can. J. Chem.* **1972**, *50*, 4034. (d) Gollnick, K.; Hartmann, H.; Paur, H. In *Oxygen and Oxy-Radicals in Chemistry and Biology*; Rodgers, M. A. J., Powers, E. L., Eds.; Academic Press: New York, 1981; pp 379−395.

(9) Hurst, J. R.; Wilson, S. L.; Schuster, G. B. *Tetrahedron* **1985**, *41*, 2191–2197.

(10) (a) Schaap, A. P.; Recher, S. G.; Faler, G. R.; Villasenor, S. R. *J. Am. Chem. Soc.* **1983**, *105*, 1691–1693. (b) Clennan, E. L.; Chen, M.-F.; Xu, G. *Tetrahedron Lett.* **1996**, *37*, 2911–2914. (c) Jefford, C. W. *Chem. Soc. Rev.* **1993**, 59–66.

(11) Stratakis, M.; Orfanopoulos, M. *Tetrahedron* **2000**, *56*, 1595–1615. See also: Alberti, M. N.; Orfanopoulos, M. *Org. Lett.* **2008**, *10*, 2465–2468, for recent studies of ene mechanisms.

(12) (a) Metiu, H.; Ross, J.; Silbey, R.; George, T. F. *J. Chem. Phys.* **1974**, *61*, 3200. (b) Valtzanos, P.; Ruedenberg, K. *Theor. Chim. Acta* **1986**, *69*, 281. (c) Valtzanos, P.; Elbert, S. T.; Ruedenberg, K. *J. Am. Chem. Soc.* **1986**, *108*, 3147. (d) Windus, T. L.; Gordon, M. S.; Burggraf, L. W.; Davis, L. P. *J. Am. Chem. Soc.* **1991**, *113*, 4356. (e) Windus, T. L.; Gordon, M. S. *Theor. Chim. Acta* **1992**, *83*, 21. (f) Yanai, T.; Taketsugu, T.; Hirao, K. *J. Chem. Phys.* **1997**, *107*, 1137. (g) Kumeda, Y.; Taketsugu, T. *J. Chem. Phys.* **2000**, *113*, 477. (h) Taketsugu, T.; Kumeda, Y. *J. Chem. Phys.* **2001**, *114*, 6973. (i) Tachibana, A.; Okazaki, I.; Koizumi, M.; Hori, K.; Yamabe, T. *J. Am. Chem. Soc.* **1985**, *107*, 1190.

(13) Singleton, D. A.; Hang, C.; Szymanski, M. J.; Greenwald, E. E. *J. Am. Chem. Soc.* **2003**, *125*, 1176–1177.

(14) Inoue, Y.; Turro, N. J. *Tetrahedron Lett.* **1980**, *21*, 4327–4330.

(15) Frisch, M. J.; Trucks, G. W.; Schlegel, H. B.; Scuseria, G. E.; Robb, M. A.; Cheeseman, J. R.; Montgomery, Jr., J. A.; Vreven, T.; Kudin, K. N.; Burant, J. C.; Millam, J. M.; Iyengar, S. S.; Tomasi, J.; Barone, V.; Mennucci, B.; Cossi, M.; Scalmani, G.; Rega, N.; Petersson, G. A.; Nakatsuji, H.; Hada, M.; Ehara, M.; Toyota, K.; Fukuda, R.; Hasegawa, J.; Ishida, M.; Nakajima, T.; Honda, Y.; Kitao, O.; Nakai, H.; Klene, M.; Li, X.; Knox, J. E.; Hratchian, H. P.; Cross, J. B.; Bakken, V.; Adamo, C.; Jaramillo, J.; Gomperts, R.; Stratmann, R. E.; Yazyev, O.; Austin, A. J.; Cammi, R.; Pomelli, C.; Ochterski, J. W.; Ayala, P. Y.; Morokuma, K.; Voth, G. A.; Salvador, P.; Dannenberg, J. J.; Zakrzewski, V. G.; Dapprich, S.; Daniels, A. D.; Strain, M. C.; Farkas, O.; Malick, D. K.; Rabuck, A. D.; Raghavachari, K.; Foresman, J. B.; Ortiz, J. V.; Cui, Q.; Baboul, A. G.; Clifford, S.; Cioslowski, J.; Stefanov, B. B.; Liu, G.; Liashenko, A.; Piskorz, P.; Komaromi, I.; Martin, R. L.; Fox, D. J.; Keith, T.; Al-Laham, M. A.; Peng, C. Y.; Nanayakkara, A.; Challacombe, M.; Gill, P. M. W.; Johnson, B.; Chen, W.; Wong, M. W.; Gonzalez, C.; and Pople, J. A. *Gaussian 03,* Gaussian, Inc.: Wallingford, CT, 2004.

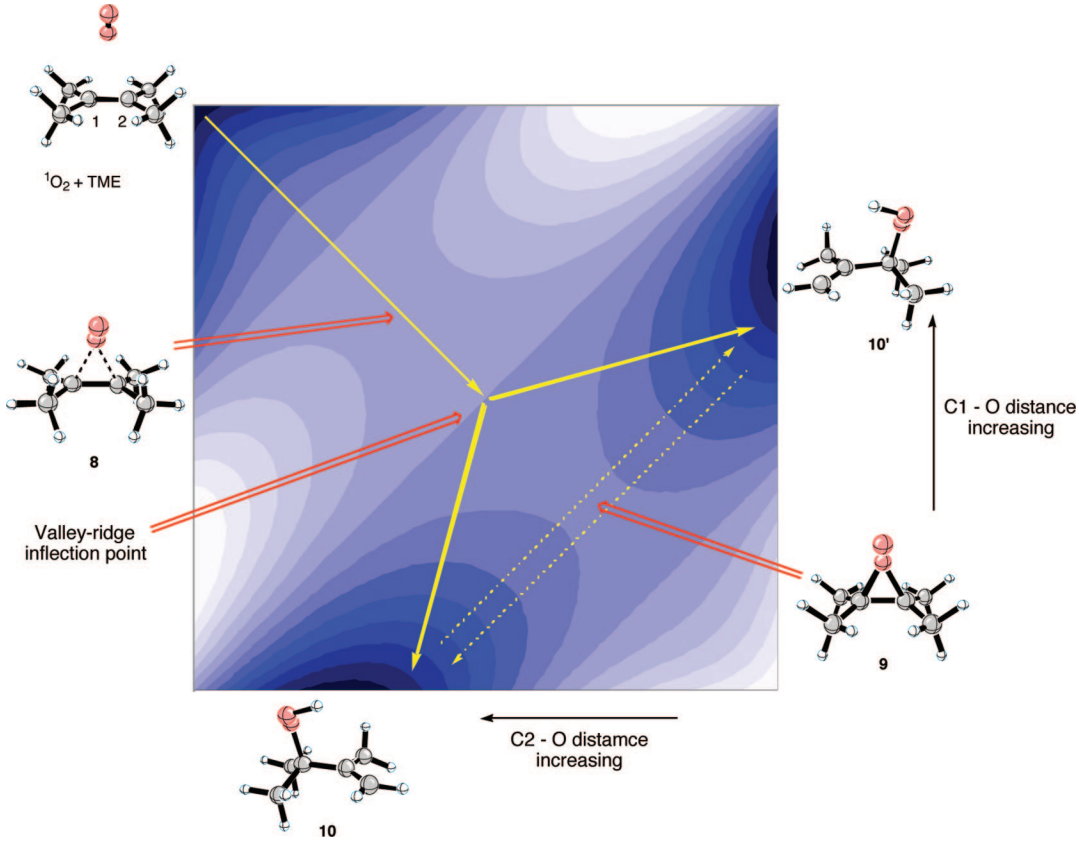

FIGURE 1. A schematic representation of the energy contour plot for the ene reaction of acyclic and flexible cyclic alkenes. Dark blue regions indicate low energy areas and light blue/white areas indicate high energy. The solid yellow arrows indicate the lowest energy path for the ene reaction and the dashed yellow arrows the notional process for which **9** would be a transition state.

is changed by substrate structure to a true two-step perepoxide intermediate mechanism.

Computational Methods

All quantum mechanical calculations were performed in Gaussian 03.[15] UB3LYP calculations employ Becke's three parameter exchange functional combined with the Lee−Yang−Parr correlation functional.[17] Unrestricted calculations utilized an initial guess in which the HOMO and LUMO were mixed in order to break the spatial symmetry of these orbitals. Vibrational corrections to enthalpy at 298 K were included, and all stationary points were validated as minima or transition states. Spin projection employed the method of Yamaguchi et al.[16] CASMP2 energies were computed and combined with vibrational corrections at the UB3LYP/6-31G* level to obtain enthalpies. Key stationary points were reoptimized at the UB3LYP/6-311G** level to ensure that they were not artifacts of the basis set selection; these data are not reported here as no deviations were found. The CASMP2 calculations involve a second order perturbation correction to a CASSCF(8,7) calculation in which the active space consisted of those orbitals that are equivalent to the following orbitals in the perepoxide: the σ and σ^* of both C−O bonds, CH σ and σ^*, and the 2p orbital at the distal O that is parallel to the C−C bond of the perepoxide ring.[18] Although it would have been preferable to include both of the 2p orbitals on the distal oxygen, it proved impossible to consistently apply this CASSCF(10,8) approach. Conformational searching employed Corina and MacroModel, the latter utilizing the OPLS force field and a Monte Carlo algorithm.[20−22]

Results and Discussion

In a previous study of the reaction of tetramethylethylene (TME) with singlet oxygen, RB3LYP/6-31G* calculations were used to optimize geometries constrained to different values of the two C−O distances that correspond to the C−O bonds of a putative perepoxide.[1,17] These geometries were subjected to CCSD(T)/6-31G* single point energy evaluations. This yielded a surface like that shown in Figure 1, which corresponds to the two-step no-intermediate mechanism. In the current study, in which reactions with *trans*-cyclooctene were to be studied, CCSD(T) calculations, even with the fairly compact 6-31G* basis set, were impractical. CASMP2/6-31G* energy evaluations were used on UB3LYP/6-31G* optimized geometries.[17,18] The change in methodology prompted a reinvestigation of the potential energy surface of the reaction of TME to ensure that the methodology reproduces the two-step no-intermediate mechanism. To this end, the surface was mapped carefully with UB3LYP/6-31G* constrained optimizations followed by full optimizations of the turning points to generate geometries for CASMP2 energy evaluations. The geometries and energies are summarized in Figure 2. In contrast to our earlier calculations

(16) Yamaguchi, K.; Jensen, F.; Dorigo, A.; Houk, K. N. *Chem. Phys. Lett.* **1988**, *149*, 537–542.
(17) (a) Becke, A. D. *J. Chem. Phys.* **1993**, *98*, 5648–5652. (b) Lee, C.; Yang, W.; Parr, R. G. *Phys. Rev. B* **1988**, *37*, 785–789. (c) Hariharan, P. C.; Pople, J. A. *Theo. Chem. Acta* **1973**, *28*, 213–222.
(18) McDouall, J. J.; Peasley, K.; Robb, M. A. *Chem. Phys. Lett.* **1988**, *148*, 183.
(19) Saunders, M.; Jiménez-Vázquez, H. A. *J. Comput. Chem.* **1990**, *11*, 848–867.
(20) *Corina*; Molecular Networks GmbH:Erlangen, Germany.
(21) Kaminski, G. A.; Friesner, R. A.; Tirado-Rives, J.; Jorgensen, W. J. *J. Phys. Chem. B* **2001**, *105*, 6474.
(22) *MacroModel*, 9.1 ed.; Schrödinger, LLC: Portland, OR, 2005.

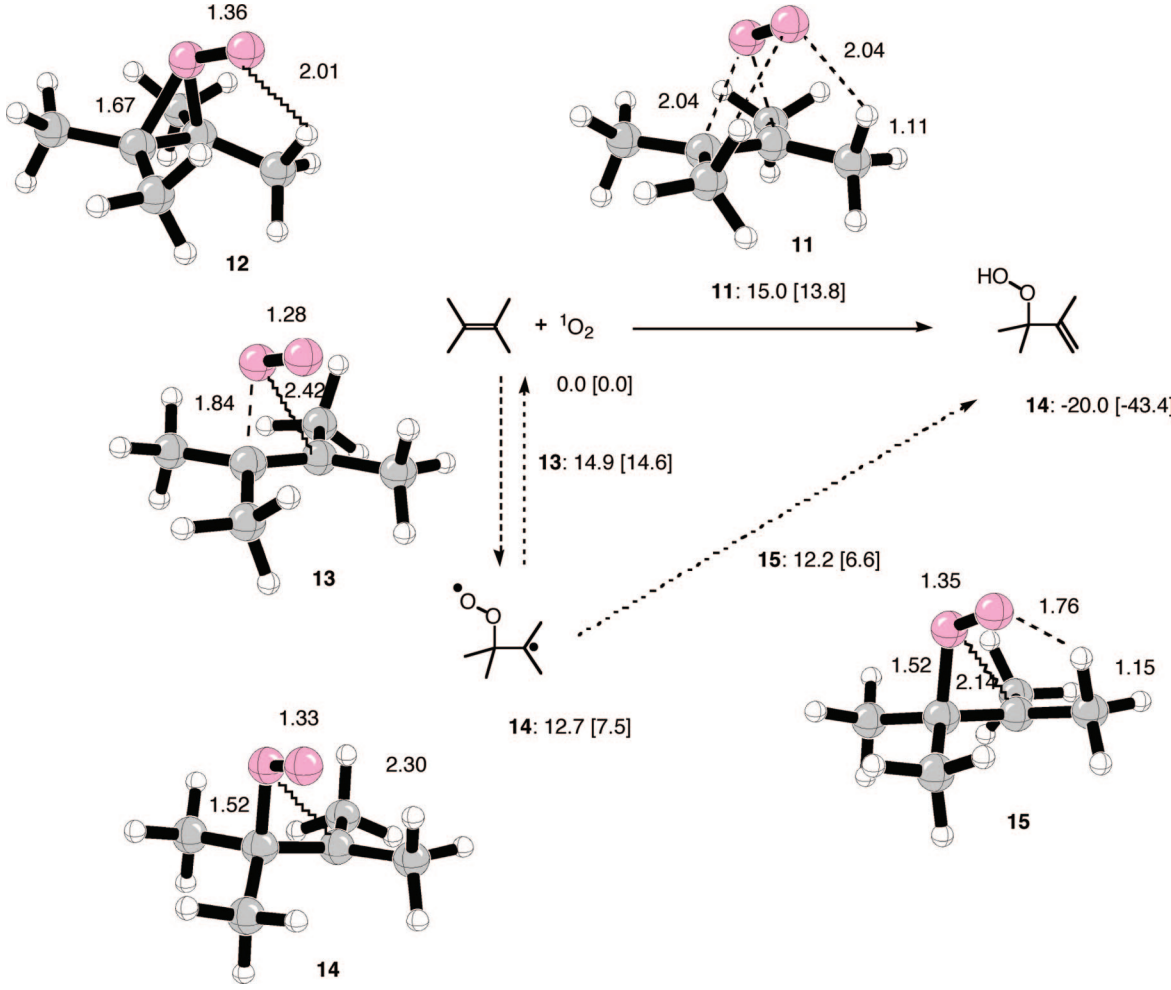

FIGURE 2. Species involved in the ene reaction between singlet oxygen and tetramethyethylene. Structures shown are optimized with UB3LYP/6-31G*. Enthalpies in kcal/mol relative to reactants are given at the UB3LYP/6-31G* level followed by the CASMP2/6-31G*//UB3LYP/6-31G* level in brackets. Distances indicated are in Å. Dashed lines indicate forming or breaking bonds; wavy lines indicate key interatomic distances.

on this surface, it was found that the UB3LYP potential energy surface actually comprises two overlaid mechanisms: one via a diradical intermediate as reported previously; the second is the two-step no-intermediate mechanism. The initial transition state for this latter process could be optimized with UB3LYP. This transition state has some open-shell character, having an $<S^2>$ value of ~0.1. It links $^1O_2$ and TME directly to ene product through a valley ridge inflection point. It is at 15.5 kcal/mol relative to reactants (13.8 kcal/mol with CASMP2). This transition state is later than that predicted by CCSD(T) calculations, which level of theory suggests both C−O distances should be 2.38 Å (2.15 Å for the reaction of *cis*-but-2-ene); in **11**, the UB3LYP transition state, these distances are 2.04 Å. A set of constrained optimizations was performed in which the two C−O distances were kept equal at values of 2.0, 2.1, 2.2, 2.3 and 2.4 Å. CASMP2 energy evaluations on these structures showed the highest energy point to be between 2.1 and 2.2 Å, better in line with the CCSD(T) calculations. The second transition state on the two-step no-intermediate path is for translation of the O−O moiety from one terminus of the alkene to the other. Although it can be optimized with UB3LYP (**12**) and is found to be at 13.4 kcal/mol relative to reactants, it is not expected that this region of the surface will actually be sampled during the reaction as it is avoided when the symmetrical path splits at the valley ridge inflection point and the reaction proceeds down one side or other of the ridge which has this transition state at its top. According to UB3LYP, the highest point on the two-step no-intermediate path is approximately equal in energy with the two regioisomeric transition states **13** and **13′** leading to diradical formation. On the electronic energy surface, the diradical formation transition state **13** leads initially to diradical **14** at 12.5 kcal/mol relative to reactants and then through a low barrier of ~0.7 kcal/mol for hydrogen abstraction (via transition state **15**) to the ene product **16**. However, when corrections to enthalpy at 298 K are included, the diradical undergoes barrierless abstraction. In line with our previous study using CCSD(T), CASMP2 energies predict an even lower barrier for abstraction which emphasizes that the diradical does not exist as an intermediate and that the two-step no-intermediate mechanism is operational. As expected, with the higher level of theory, CASMP2, the diradical forming transition state **13** is somewhat higher in energy than the symmetrical transition state **11** and presumably now represents a point up the sides of the valley that has transition state **11** at its center.

The same method described above has been applied to the reaction of *trans*-cyclooctene. This reaction has been studied experimentally by Inoue and Turro[14] and subsequently by Poon, Pringle, and Foote.[2] In the study of Poon et al., trapping with $P(OPh)_3$ was used to detect the existence of a perepoxide in the reaction mixture. In the absence of the trapping agent, a number of products form, including *cis*-cyclooctene **17**, *cis*- and *trans*-epoxides (**18** and **19**, respectively), ene product **20**, and

SCHEME 1. Experimentally Observed Products of the Reaction of Singlet Oxygen with *trans*-Cyclooctene

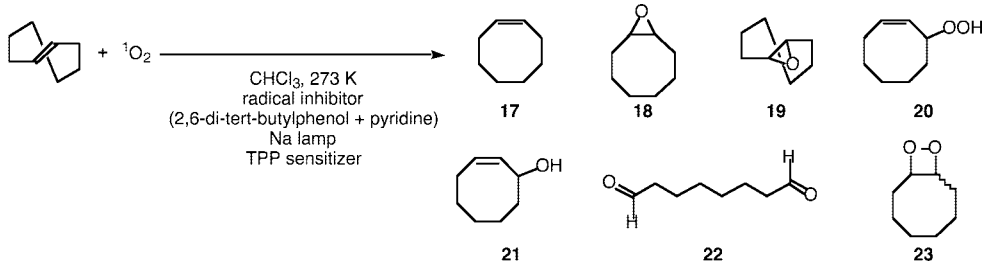

TABLE 1. Concentrations of Key Species at Different Times and under Different Conditions in the Reaction of Singlet Oxygen with *trans*-Cyclooctene[a]

reaction time (min)	initial [*trans*-cyclooctene]	initial [$P(OPh)_3$]	[**17**]	[*trans*-cyclooctene]	[**18**]	[**19**]	[**21**]	[**20**]	[**22**]	[$P(OPh)_3$]	[phosphate]
30	100	0	6.5	83	1.3	0.348	3.1	6.7	0	0	0
90	100	0	3.2	58	2.7	0.8	6.2	14.6	0.4	0	0
150	20	0	0.34	4	0.6	0.26	4		0	0	0
150	20	4.7	0.24	3.4	0.73	1.1	3.7		0	0	1.6
150	20	9.3	0.2	3.4	0.59	2	3.2		0	0.24	3.5
150	20	19.1	0.17	3.6	0.49	3.3	2		0	4.9	5
150	20	29.2	0.15	3.3	0.28	4.1	1.7		0	11	6.5
150	20	39.4	0.13	3.5	0.4	4.4	1.2		0	19	7
150	62	0	0.69	24	1.1	0.36	5.4		0	0	0
150	62	4.9	0.42	23	1.3	1.6	5.2		0	0	1.9
150	62	9.8	0.35	23	1.1	3.4	5.6		0	0	3.9
150	62	19.3	0.15	31	0.59	3.6	2.1		0	5	5.1
150	62	29.5	0.21	24	0.74	7.7	3.1		0	5.4	8.7
150	62	39.4	0.18	24	0.64	8.5	2.3		0	12	9.7

[a] Reproduced from ref 2.

its reduced alcohol form **21** (Scheme 1). The dialdehyde **22**, arising from degradation of the dioxetane **23** reported by Inoue and Turro, was detected at far lower levels by Poon et al. The relative amounts of each of these products under varying reaction conditions are reproduced from ref 2 in Table 1. The same reactions were run with differing levels of $P(OPh)_3$ present, and the results from these studies are also summarized in Table 1.

The formation and trapping of both *trans*-epoxide **19** and *cis*-configured alkene and epoxide hints at the intermediacy both of perepoxide and open chain intermediates. Therefore an expansive characterization of the potential energy surface was undertaken including the rotation of possible open chain intermediates.

As previously described,[19] *trans*-cyclooctene has only a small number of low energy conformations available. The 3D structure generator Corina was employed to identify low lying conformations.[20] Subsequent optimization with RB3LYP/6-31G* yielded two conformations differing in energy by 5.6 kcal/mol. A model fused 3,8 ring system was used to generate conformations that a perepoxide in this system might adopt using both Corina (which generated only one conformation) and the OPLS force field in a Monte Carlo conformational search that generated a range of conformations, some of which were identical.[21,22] Subsequent optimizations with B3LYP revealed that all conformations optimized to perepoxide minima in direct contrast to the case for other alkenes, where the closest such species is a transition state and most attempts to optimize a perepoxide yield ene product. It was ascertained during later study that the lowest energy conformation of the cyclooctene ring is different for perepoxide and diradicals. Each point studied which has a *trans* configuration about the initial *trans*-alkene was optimized in a conformation corresponding to the lowest energy in both the perepoxide and also in the diradical. The lowest energy is reported throughout with the labels **a** and **b** designating whether it is in the perepoxide or diradical conformation, respectively.

A similar exercise with *trans*-cyclononene showed that of 10 generated conformations, six optimized to perepoxides, whereas the remainder directly optimized to ene product. This suggests that the perepoxide is a minimum but will be hard to detect experimentally since there exist conformations that undergo barrierless reaction to yield ene product.

The perepoxide **24a** of *trans*-cyclooctene was used as the starting point for a systematic scan of the C−O distances corresponding to the two C−O bonds in the perepoxide. This search revealed that at the B3LYP/6-31G* level (both restricted and unrestricted), the lowest energy path linking $^1O_2$ + *trans*-cyclooctene to perepoxide **24a** involves the intermediacy of an open chain intermediate. As in the reactions of nitroso compounds and triazolinediones, these open shell diradicals are highly polar in character and therefore have much in common with zwitterionic intermediates. Such intermediates are well described as polarized diradicals.[4] The perepoxide **24** is linked to two regioisomeric polarized diradicals (PDs) **25** and **26** by two transition states **27** and **28**, and the PDs in turn may dissociate through transition states **29** and **30**. The energetics calculated for these species are shown in Figure 3.

The key stationary points identified during this initial search of the potential energy surface are summarized in Figure 3. Although the energies are discussed in detail in subsequent sections, it is curious to note that UB3LYP and CASMP2 differ in which region of the potential energy surface is the highest. While UB3LYP predicts that the rate of PE formation should be limited by diradical cyclization (and be endothermic), CASMP2 predicts that it is the initial diradical formation step that is rate-limiting and that the PE is lower in energy than reactants. The lower barriers for diradical formation with

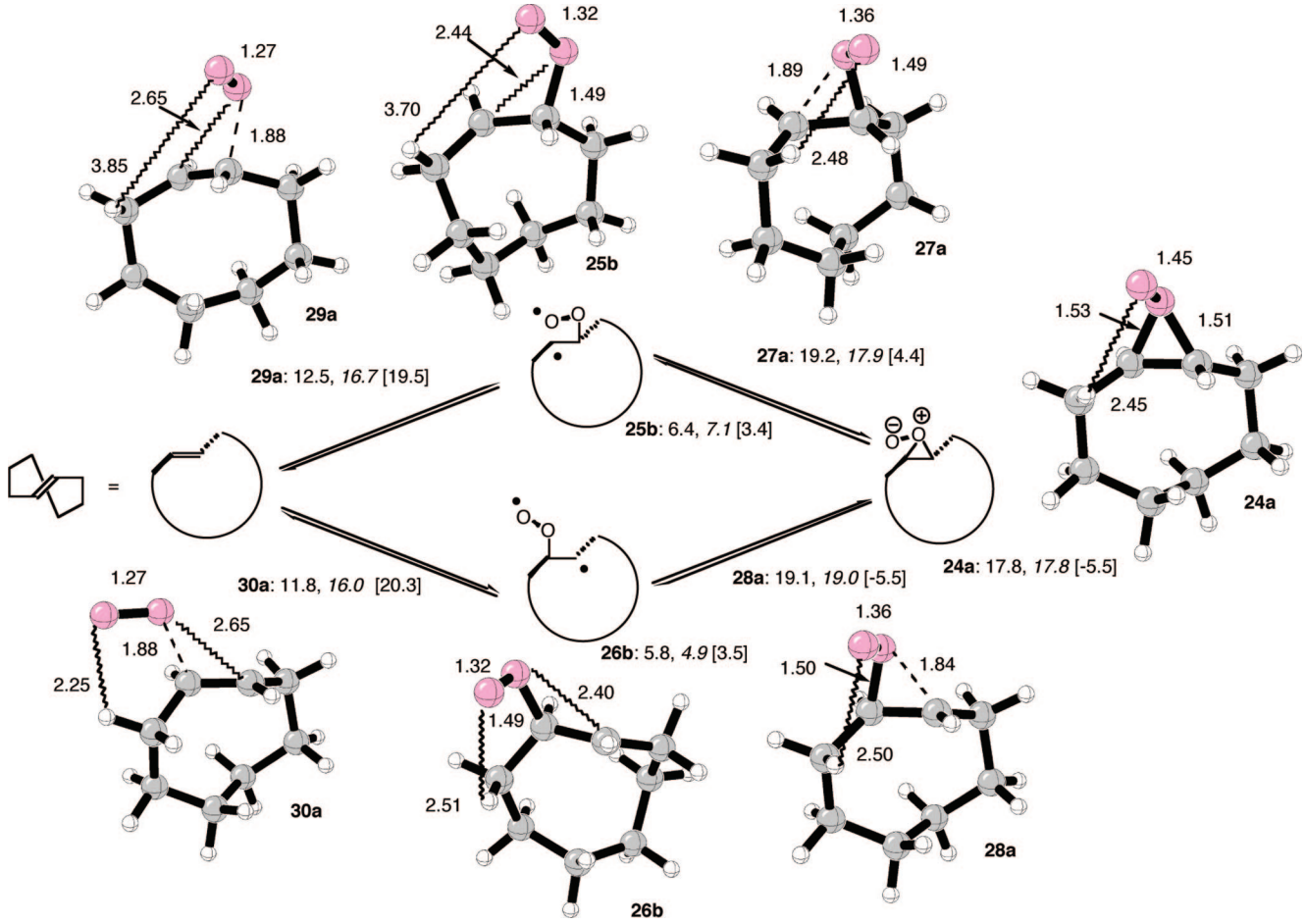

FIGURE 3. Species involved in the formation of perepoxide from singlet oxygen and *trans*-cyclooctene. Geometries shown were optimized at the UB3LYP/6-31G* level. Energies indicated are enthalpies at 298 K at the UB3LYP/6-31G* level followed by spin projected values in italics and CASMP2/6-31G* single point energies in brackets. Distances shown are in Å. Dashed lines indicate forming or breaking bonds; wavy lines indicate key interatomic distances.

UB3LYP are significantly due to spin contamination. When the enthalpy of the uncontaminated singlet is obtained by projection,[16] these barriers are raised by approximately 4 kcal/mol.

Polarized diradicals **25** and **26** might also be linked by rotation about the C−O bond and ought also to access a third conformer, **31**, by this same rotation. This is the case, and these conformers are approximately equienergetic and have barriers to rotation of less than 1.2 kcal/mol (see Figure S3 in Supporting Information). This suggests rapid rotation and conformational equilibration among three more or less equienergetic conformations. This is in contrast to the case for the equivalent PDs in the reaction of nitroso compounds where the barriers to rotation are found to be 3−5 kcal/mol and are of a comparable magnitude to barriers for other processes.[23] Interestingly, the O•OCC• dihedral in the dissociation transition states for these diradicals takes values that are intermediate between those in the diradical minima. This suggests that the diradical formation from cyclooctene and singlet oxygen involves a reaction path bifurcation similar to that illustrated in Figure 1. After the initial transition state, one of the closest two diradical minima might form depending on dynamic behavior around an inflection point on the surface.

Spin projection energies indicated that triplet diradicals are lower in energy than singlets in some conformations of the PD. Although it cannot be studied with the techniques applied here, it is possible that spin transitions may contribute to the observed outcome in the experiments. The triplet diradicals have no barrier to dissociation so this would enhance the rate at which reversion to cyclooctene (both *trans*-cyclooctene from **25**, **26**, and **31** but also *cis*-cyclooctene from **36** and **40**, described later) takes place.

The next three parts of the surface to be explored were those involving rotation about the C−C bond in the PDs **25b**, **26b**, and **31b**. This study was done by driving the dihedral in these PDs. The lowest energy path that accesses the *cis*-configured part of the surface links from PD **31b** to the PD **40** (Figure 4). The results of all of these studies are summarized in Figures S4 and S5 in Supporting Information. Diradical **40** has three options open to it: dissociation to form *cis*-cyclooctene, cyclization to form perepoxide, or hydrogen abstraction to yield ene product. Internal rotation of the PD is key to achieving some of these processes and is expected to be facile, by analogy with rotation in **25/26/31**. The key stationary points and energetics are summarized in Figure 4.

The relative energies of **31** and **40** indicate that much of the strain inherent in *trans*-cyclooctene has been relieved upon diradical formation such that rotation into a *cis* arrangement leads to diradicals close in energy (<2.5 kcal/mol different) contrasting starkly with the >10 kcal/mol energy difference

(23) Leach, A. G.; Houk, K. N. *Org. Biomol. Chem.* **2003**, *1*, 1389–1403.

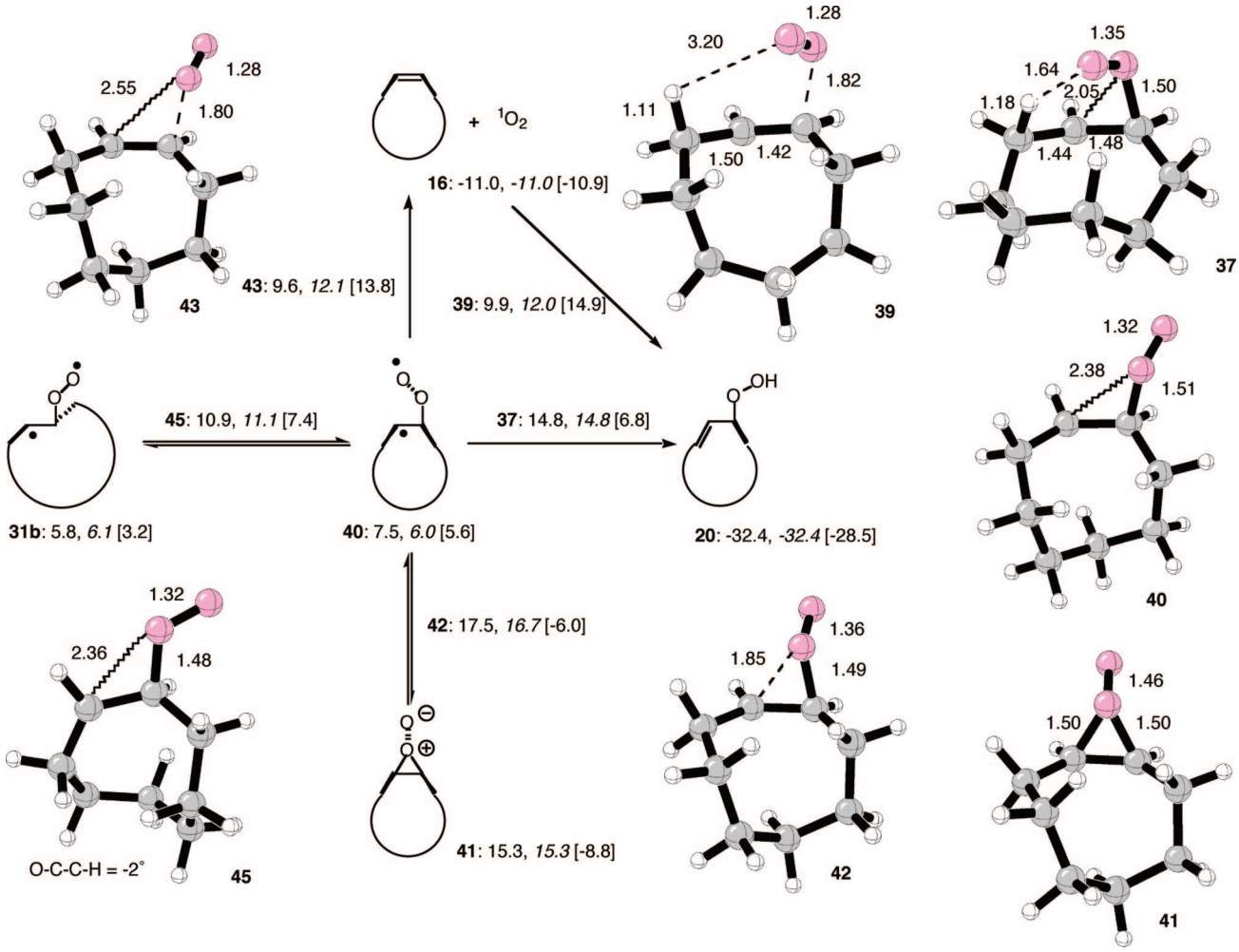

FIGURE 4. Internal rotation of a polarized diradical to a *cis*-configured polarized diradical and reactions that are accessible from that species. Geometries shown were optimized at the UB3LYP/6-31G* level. Energies indicated are enthalpies at 298 K at the UB3LYP/6-31G* level followed by spin projected values in italics and CASMP2/6-31G* single point energies in brackets. Distances shown are in Å. Dashed lines indicate forming or breaking bonds; wavy lines indicate key interatomic distances.

between *cis*- and *trans*-cyclooctene. Polarized diradical **40** can cyclize to the unproductive bystander perepoxide **41**. Rotation about the CC bond in **26b** or rotation about the C−O bond in **40** gives a *cis*-arranged conformation poised to undergo hydrogen abstraction. As expected in the more flexible *cis*-arranged ring when the oxygen is oriented toward an abstractable proton, a perepoxide cannot be optimized and transition state **37** for hydrogen abstraction is obtained. The diradical **40** can also dissociate to yield *cis*-cyclooctene through transition states like **43**.

The portion of the surface illustrated in Figure 4 indicates a potential pathway for the ene reaction of *cis*-cyclooctene through **43**, **40**, and **37**. However, Poon et al.'s studies suggest that *cis*-cyclooctene, like most alkenes able to undergo ene reaction, does not yield experimental evidence of any intermediates.[2] This is consistent with the two-step no-intermediate reaction. In line with this, conformational searching and optimization with RB3LYP/6-31G* indicated that there are a number of conformations of perepoxide for *cis*-cyclooctene that cannot be optimized as minima and instead optimize directly to the ene product. This is part of the fingerprint for reactions that do not pass through such an intermediate. A transition state, **39**, in one of these conformations that do not sustain perepoxides was optimized and found to be 9.9 kcal/mol above *trans*-cyclooctene and $^1O_2$, or 21.0 kcal/mol relative to *cis*-cyclooctene and $^1O_2$, with RB3LYP. It is assumed that the reaction of *cis*-cyclooctene proceeds through an ensemble of transition states like **39** through the two-step no-intermediate reaction directly to ene product. By contrast, access to the *cis*-arranged ring from the *trans* arrangement delivers at least some of the polarized diradical in conformations like **40**, which undergo facile (likely barrierless according to CASMP2) cyclization to form *cis*-perepoxide. This is consistent with the observation of *cis*-epoxide in the reaction of *trans*-cyclooctene but not with *cis*-cyclooctene.

The final part of the surface to be explored was that corresponding to the final step of the ene reaction, the abstraction of one of the allylic hydrogens. As observed in related cases previously,[24] a scan linking the perepoxide to the ene product revealed that although the formal lowest energy path linking the two goes through PD **25**, dynamic motion across the surface may be able to bypass the minimum itself and access **46** directly. There are likely to be a number of such trajectories whose maximum in energy is close to that on the trajectories that do sample the PD. The geometry of **46a** in Figure 5 shows substantial lengthening of the C−H bond and a relatively short

(24) Black, K. A.; Leach, A. G.; Kalani, M. Y. S.; Houk, K. N. *J. Am. Chem. Soc.* **2004**, *126*, 9695–9708.

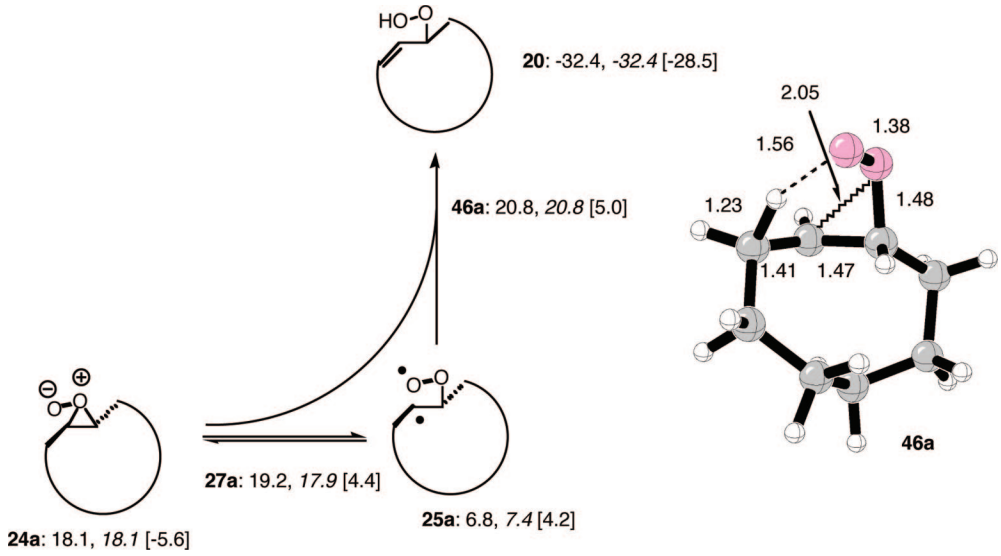

FIGURE 5. Species linking perepoxides to ene product. Geometries shown were optimized at the UB3LYP/6-31G* level. Energies indicated are enthalpies at 298 K at the UB3LYP/6-31G* level followed by spin projected values in italics and CASMP2/6-31G* single point energies in brackets. Distances shown are in Å. Dashed lines indicate forming or breaking bonds; wavy lines indicate key interatomic distances.

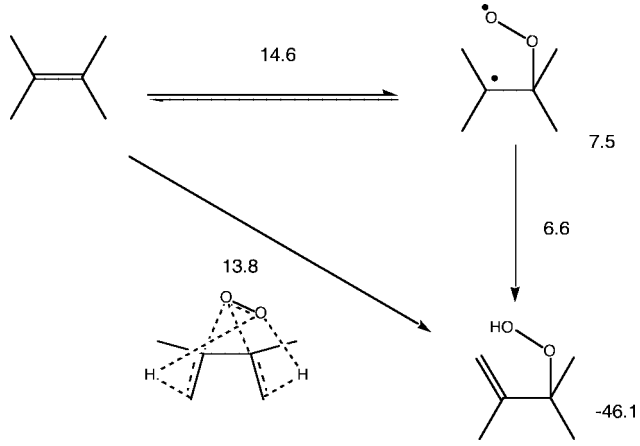

FIGURE 6. Summary of key points computed in the ene reaction of TME with singlet oxygen. The diradical pathway is shown to not be active. The energies indicated are CASMP2 enthalpies in kcal/mol.

O−H distance. These lengths are closer to those of the reactant than the product indicating an early transition state, as ought to be expected for this highly exothermic step.

The various fragments of the potential energy surface can be drawn together and are summarized for TME in Figure 6 and *trans*-cyclooctene in Figure 7. In these figures, the key energetics with CASMP2 only are shown. Figure 6 demonstrates that for TME, whereas UB3LYP permitted structures corresponding to a diradical stepwise pathway to be optimized, at the CASMP2 level they represent a path that passes through one energetic highpoint and then continues downhill without interruption to the ene product. This is a pathway that does not actually involve an intermediate.

By contrast, as shown in Figure 7, the strain inherent in the abstraction transition state **46** ensures that not only are the polarized diradicals now minima (albeit with very low barriers to various rotations and to abstraction), but the perepoxide can also be reached. The barrier to abstraction means that the surface in Figure 1 is effectively modified with a wall restricting access to the ene product and therefore making open chain intermediates and the perepoxide minima. The consequences of this are that other manifolds for reaction open up. Some conformations of the polarized diradical (**26**) may undergo barrierless cyclization to give perepoxide such that it is the internal rotation barrier that limits the rate of its formation from the lowest energy conformation **31**. This is the source of **19** in the trapping experiments. That this cyclization has the lowest barrier for reactions open to the PD is consistent with the observation that interception of the PE with phosphite decreases the amount of alkene isomerization and ene product formation observed.

The PDs can also undergo internal rotation, which enables access to *cis*-configured species that may dissociate to yield *cis*-cyclooctene itself or cyclization to give *cis*-perepoxide, likely responsible for the observation of **18** in the reaction mixture. The enthalpies reported here indicate dissociation to be a poorly competitive part of the surface. The entropic advantage associated with the dissociation and spin flipping into a triplet diradical may further contribute to the observed amount of **17** during the reactions.

The energetics in Figure 7 suggest that the PDs play the role of a caldera, often identified before for similar species involved in stepwise pericyclic reactions.[25] They are formed endothermically and have low barriers to a variety of reactions, so they are impossible to detect but it is motion in this part of the surface that will dictate the outcome of the reaction that is observed. The species that is formed by falling off the caldera is not independent of the point of entry to the caldera and hence the energies reported here may not be the exclusive determinant of the outcome of the reaction. In this case, the initially formed PD permits access to PE, ene product and *cis*-configured species.

The calculations indicate that the *trans*- and *cis*-perepoxides are minima and indeed may be lower in energy than reactants and hence readily intercepted. They are substantially higher in energy than the ene product and have relatively small barriers to yield that product. They are also higher in energy than *cis*-cyclooctene and hence the observation of *cis*-cyclooctene as a

(25) (a) Doering, W. v. E.; Cheng, X.; Lee, K.; Lin, Z. *J. Am. Chem. Soc.* **2002**, *124*, 11642–11652. (b) Doering, W. v. E.; Barsa, E. A. *J. Am. Chem. Soc.* **2004**, *126*, 12353–12362. (c) Doubleday, C.; Suhrada, C. P.; Houk, K. N. *J. Am. Chem. Soc.* **2006**, *128*, 90–94. (d) Suhrada, C. P.; Houk, K. N. *J. Am. Chem. Soc.* **2002**, *124*, 8796–8797.

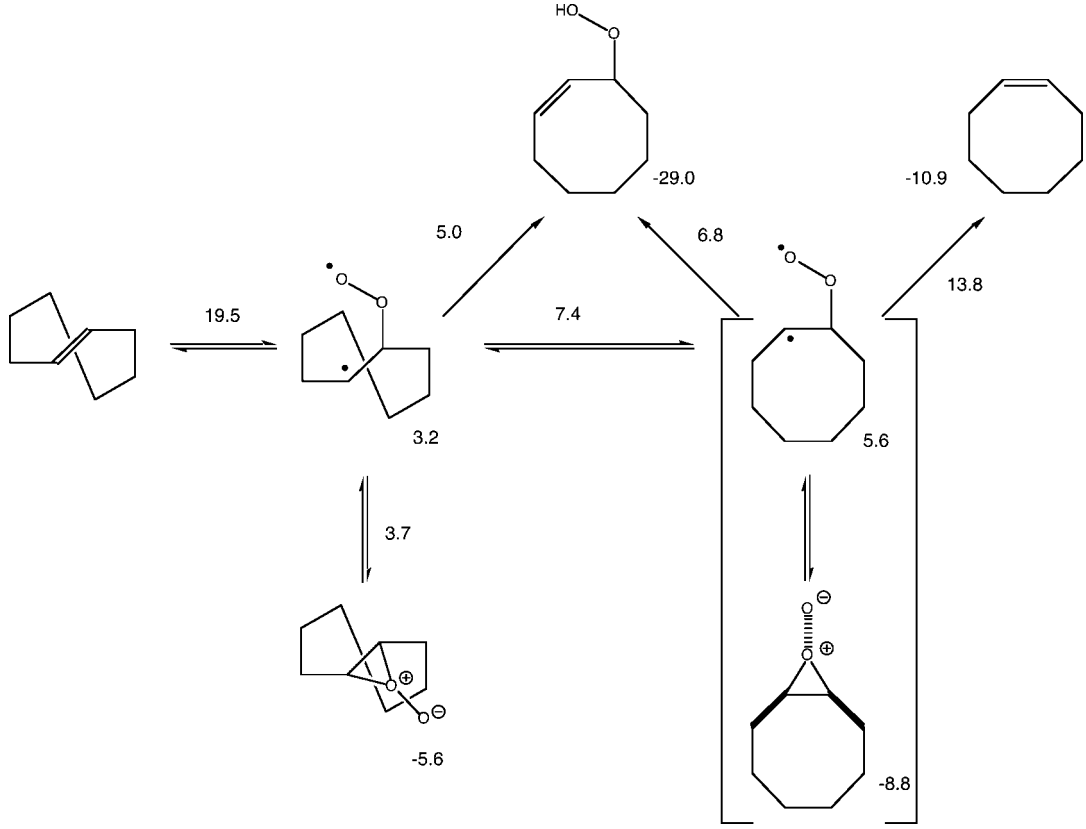

FIGURE 7. Summary of the key points in the reaction of singlet oxygen with *trans*-cyclooctene. This contrasts sharply with that for TME and involves a number of intermediates, including two configurations of perepoxides. Polarized diradicals are a higher energy caldera that facilitate the internal rotations that lead to the observed product outcomes. Enthalpies shown are CASMP2/6-31G* values.

reaction product. There is an independent route to ene product through the usual two-step no-intermediate mechanism for *cis*-cyclooctene.

Conclusions

Studies using UB3LYP geometry optimizations with CASMP2 single point energy evaluations reveal that in contrast to the reaction of most normal alkenes which undergo a two-step no-intermediate reaction, *trans*-cyclooctene imposes a barrier to hydrogen abstraction thanks to the large strain in the transition state for this process. This barrier has the consequence of enabling both open chain polarized diradicals and perepoxides to exist. The open chain species act as a relatively flat caldera like region in which internal rotation, cyclization to perepoxides and hydrogen abstraction are the outcome of falling off in various directions. The energetic landscape reported is consistent with the experimental outcome in which ene product, products derived from perepoxides, and products arising from alkene isomerization are all observed.

Supporting Information Available: Summary of all optimized stationary points, all geometries and energies at B3LYP/6-31G* and CASMP2/6-31G* levels. This material is available free of charge via the Internet at http://pubs.acs.org.

JO8016154